AD-A037 755 NAVAL UNDERSEA CENTER SAN DIEGO CALIF F/G 9/4
PRINCIPLES AND APPLICATIONS OF ADAPTIVE FILTERS: A TUTORIAL REV--ETC(U)
MAR 77 J M MCCOOL, B WIDROW
UNCLASSIFIED NUC-TP-530 NL

1 OF 1
AD A037755

END
DATE FILMED
4-77

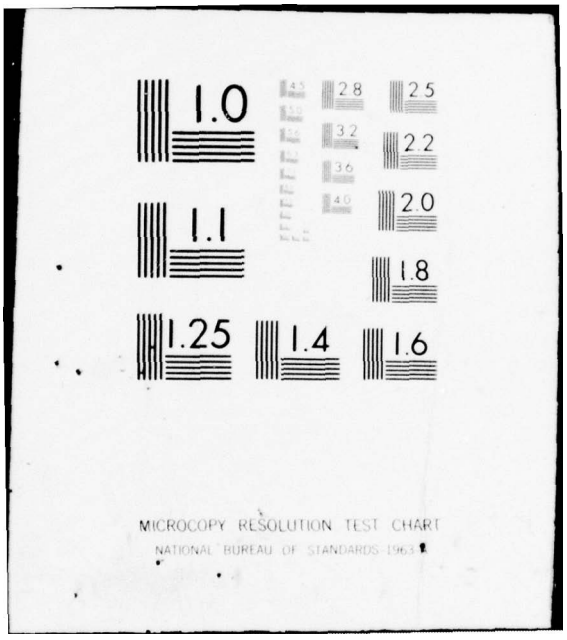
1.0
1.1
1.25
1.4
1.6
1.8
2.0
2.2
2.5
2.8
3.2
3.6
4.0
MICROCOPY RESOLUTION TEST CHART
NATIONAL BUREAU OF STANDARDS-1963-A

NUC TP 530

PRINCIPLES AND APPLICATIONS OF ADAPTIVE FILTERS: A TUTORIAL REVIEW

by

John M. McCool

FLEET ENGINEERING DEPARTMENT

Bernard Widrow

STANFORD UNIVERSITY

March 1977

NAVAL UNDERSEA CENTER, SAN DIEGO, CA. 92132

AN ACTIVITY OF THE NAVAL MATERIAL COMMAND

R. B. GILCHRIST, CAPT, USN
Commander

HOWARD L. BLOOD, PhD
Technical Director

ADMINISTRATIVE INFORMATION

This report is an expanded version of a paper presented at the International Specialist Seminar on the Impact of New Technologies in Signal Processing sponsored by the British Institution of Electrical Engineers and held at Aviemore, Scotland, 20–24 September 1976.

Released by
D. A. KUNZ, Head
Fleet Engineering Department

ACKNOWLEDGMENT

The authors are indebted to Robert Fraser of the Naval Undersea Center for assistance in preparing this report.

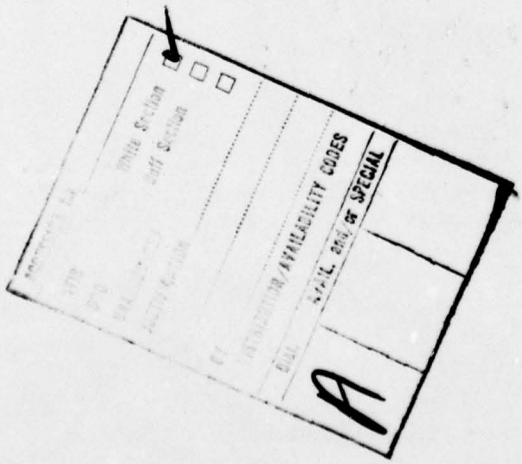

UNCLASSIFIED

SECURITY CLASSIFICATION OF THIS PAGE (When Data Entered)

REPORT DOCUMENTATION PAGE	READ INSTRUCTIONS BEFORE COMPLETING FORM
1. REPORT NUMBER: TP-530 (14 NUC)	2. GOVT ACCESSION NO. / 3. RECIPIENT'S CATALOG NUMBER
4. TITLE (and Subtitle): PRINCIPLES AND APPLICATIONS OF ADAPTIVE FILTERS: A TUTORIAL REVIEW (6)	5. TYPE OF REPORT & PERIOD COVERED / 6. PERFORMING ORG. REPORT NUMBER
7. AUTHOR(s): John M. McCool, Bernard Widrow (10)	8. CONTRACT OR GRANT NUMBER(s)
9. PERFORMING ORGANIZATION NAME AND ADDRESS: Naval Undersea Center, San Diego, CA. 92132	10. PROGRAM ELEMENT, PROJECT, TASK AREA & WORK UNIT NUMBERS
11. CONTROLLING OFFICE NAME AND ADDRESS	12. REPORT DATE (11) Mar 77 / 13. NUMBER OF PAGES: 36 (12) 39 pp
14. MONITORING AGENCY NAME & ADDRESS (if different from Controlling Office)	15. SECURITY CLASS. (of this report): Unclassified / 15a. DECLASSIFICATION/DOWNGRADING SCHEDULE

16. DISTRIBUTION STATEMENT (of this Report)

Approved for public release; distribution unlimited.

17. DISTRIBUTION STATEMENT (of the abstract entered in Block 20, if different from Report)

18. SUPPLEMENTARY NOTES

390 458

19. KEY WORDS (Continue on reverse side if necessary and identify by block number)

20. ABSTRACT (Continue on reverse side if necessary and identify by block number)

This report reviews the characteristics of a class of adaptive filters useful in signal processing and other applications where the properties of the signal are unknown or variable with time. The basic element of these filters is the adaptive linear combiner, which weights (adjusts the gain of) and sums a set of input signals to form a single output signal. The weighting process is governed by a recursive algorithm that seeks to minimize the mean square of the difference between the combiner's output and a "desired response" (training signal). It is shown that

OVER

DD FORM 1 JAN 73 1473 EDITION OF 1 NOV 65 IS OBSOLETE

UNCLASSIFIED

SECURITY CLASSIFICATION OF THIS PAGE (When Data Entered)

bpg

20. Continued

for statistically stationary inputs the mean-square difference is a quadratic function of the weight values, allowing the minimum to be sought by gradient estimation and other similar techniques. Expressions are given that define the relationship between rate of adaptation and deviation from optimal performance due to noise in the gradient estimation process for the Widrow-Hoff LMS algorithm. Methods of deriving the inputs to the combiner are described, including the use of a tapped delay line to form an adaptive transversal filter. Experimental results obtained by computer simulation are presented that show the ability of the adaptive transversal filter to model an unknown network or physical system; to reduce or eliminate intersymbol interference in multipath communication channels; to reduce or eliminate periodic interference in electrocardiography and broadband interference in the sidelobes of an antenna array; and to separate periodic and broadband signals and detect very low level periodic signals.

SUMMARY

This report reviews the characteristics of a class of adaptive filters useful in signal processing and other applications where the properties of the signal are unknown or variable with time. The basic element of these filters is the adaptive linear combiner, which weights (adjusts the gain of) and sums a set of input signals to form a single output signal. The weighting process is governed by a recursive algorithm that seeks to minimize the mean square of the difference between the combiner's output and a "desired response" (training signal). It is shown that for statistically stationary inputs the mean-square difference is a quadratic function of the weight values, allowing the minimum to be sought by gradient estimation and other similar techniques. Expressions are given that define the relationship between rate of adaptation and deviation from optimal performance due to noise in the gradient estimation process for the Widrow-Hoff LMS algorithm. Methods of deriving the inputs to the combiner are described, including the use of a tapped delay line to form an adaptive transversal filter. Experimental results obtained by computer simulation are presented that show the ability of the adaptive transversal filter to model an unknown network or physical system; to reduce or eliminate intersymbol interference in multipath communication channels; to reduce or eliminate periodic interference in electrocardiography and broadband interference in the sidelobes of an antenna array; and to separate periodic and broadband signals and detect very low level periodic signals.

CONTENTS

INTRODUCTION

The term "filter" may be applied to any device or system that processes incoming signals or other data in such a way as to smooth or classify them, predict future values, or eliminate interference. Adaptive filters are devices that automatically adjust their own parameters and seek to optimize their performance according to a specific criterion. Though somewhat more difficult to design, analyze, and build than fixed filters, they offer the potential of substantial improvements in performance when signal properties are unknown or variable with time.

This report is concerned with a particular class of adaptive filters and with their application to problems primarily in the field of signal processing. These filters have as their basic element a device that is versatile and relatively easy to implement in hardware or software. This device, the adaptive linear combiner, is treated first in the following pages. The Widrow-Hoff LMS algorithm, the most efficient of a number of algorithms available for governing its operation, is considered next. Methods of deriving input signals for the combiner to form adaptive filters are then considered, with emphasis on the use of a tapped delay line to form an adaptive transversal filter. The applications subsequently presented show how the adaptive transversal filter can be used to perform modeling and equalization tasks, cancel interference, and detect low-level signals.

THE ADAPTIVE LINEAR COMBINER

The adaptive linear combiner, illustrated in figure 1, is the basic element of the adaptive filters considered in this report.[1] A set of n measurements $x_i(t)$ is sampled to form n sampled measurements x_{ij}, where j is the time index. Each measurement is multiplied by a corresponding weighting coefficient w_i, and the weighted measurements are summed to form an output y_j. This output is compared with a desired response d_j to form an error signal ϵ_j. The objective is to choose the weighting coefficients in such a way as to minimize the error signal and find the weighted sum of input signals that best matches the desired response.[2]

---

[1] *The combiner is linear only when the weighting coefficients defined below are fixed. Adaptive systems, like all systems whose characteristics change with the characteristics of their input signals, are by nature nonlinear.*

[2] *The earliest adaptive systems (ref. 1, 2) and many current systems, particularly adaptive antenna arrays (ref. 3), employ as weights balanced modulators driven by an integrator or a narrow low- or band-pass filter. These systems, although apparently different from systems based on the adaptive linear combiner, have similar characteristics and can be considered as an alternative and sometimes preferable implementation.*

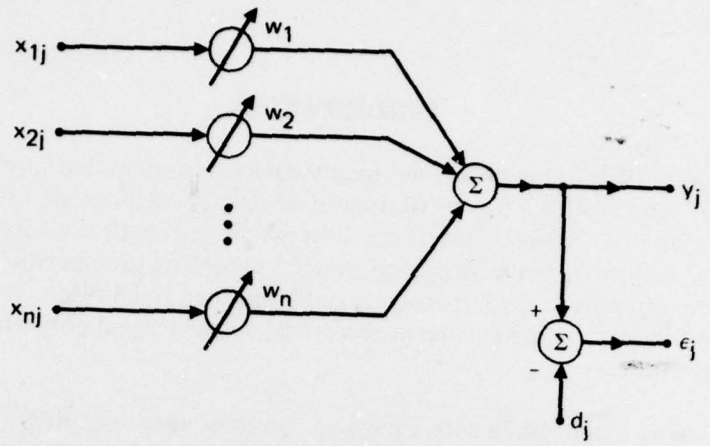

Figure 1. Adaptive linear combiner.

The jth output signal of the combiner is given by

$$y_j = \sum_{i=1}^{n} w_i x_{ij}, \tag{1}$$

which may be written in matrix form as

$$y_j = \underset{\sim}{X}_j^T \underset{\sim}{W} = \underset{\sim}{W}^T \underset{\sim}{X}_j, \tag{2}$$

where $\underset{\sim}{X}_j$ and $\underset{\sim}{W}$ are vectors of the measurements and weights respectively. The error signal is given by

$$\epsilon_j = d_j - y_j = d_j - \underset{\sim}{W}^T \underset{\sim}{X}_j. \tag{3}$$

The square of the error is

$$\epsilon_j^2 = d_j^2 - 2d_j \underset{\sim}{X}_j^T \underset{\sim}{W} + \underset{\sim}{W}^T \underset{\sim}{X}_j \underset{\sim}{X}_j^T \underset{\sim}{W}. \tag{4}$$

The mean square error, obtained by taking the expected value of equation (4), is

$$E\left[\epsilon_j^2\right] = E\left[d_j^2\right] - 2E\left[d_j \underset{\sim}{X}_j^T\right] \underset{\sim}{W} + \underset{\sim}{W}^T E\left[\underset{\sim}{X}_j \underset{\sim}{X}_j^T\right] \underset{\sim}{W}. \tag{5}$$

Defining the vector $\underset{\sim}{P}$ as the cross correlation between the desired response (a scalar) and $\underset{\sim}{X}$ then yields

$$\underset{\sim}{P} \triangleq E\left[d_j \underset{\sim}{X}_j\right] = E\left[d_j x_{1j}, d_j x_{2j}, \ldots, d_j x_{nj}\right]^T. \tag{6}$$

The input correlation matrix $\underset{=}{R}$ is defined as

$$\underset{=}{R} \triangleq E\left[\underset{\sim}{X}_j \underset{\sim}{X}_j^T\right] = E\begin{bmatrix} x_{1j}x_{1j} & x_{1j}x_{2j} & \cdots \\ x_{2j}x_{1j} & x_{2j}x_{2j} & \cdots \\ \vdots & \vdots & \\ \vdots & \vdots & \\ \vdots & \vdots & \\ & \cdots & x_{nj}x_{nj} \end{bmatrix} \tag{7}$$

The mean square error can thus be expressed as

$$E\left[\epsilon_j^2\right] = E\left[d_j^2\right] - 2\underset{\sim}{P}^T\underset{\sim}{W} + \underset{\sim}{W}^T\underset{=}{R}\underset{\sim}{W}. \tag{8}$$

Note that for stationary inputs the error is a quadratic function of the weights that can be pictured as a concave hyperparaboloidal surface, a function with a unique minimum. Adjusting the weights to minimize the error is accomplished by descending along this surface with the objective of finding its minimum. Gradient methods are commonly used for this purpose.

The gradient $\underset{\sim}{\nabla}$ of the error function is obtained by differentiating equation (8) with respect to the weight vector $\underset{\sim}{W}$:

$$\underset{\sim}{\nabla} \triangleq \left\{\frac{\partial E\left[\epsilon_j^2\right]}{\partial w_1}, \ldots, \frac{\partial E\left[\epsilon_j^2\right]}{\partial w_n}\right\}^T = -2\underset{\sim}{P} + 2\underset{=}{R}\underset{\sim}{W}. \tag{9}$$

The optimal weight vector $\underset{\sim}{W}^*$, generally called the Wiener weight vector, is obtained by setting the gradient of the mean square error function to zero:

$$\underset{\sim}{W}^* = \underset{=}{R}^{-1}\underset{\sim}{P}. \tag{10}$$

This equation is a matrix form of the Wiener-Hopf equation (ref. 4, 5). The minimum mean square error (mse) can be expressed as follows by substituting equation (10) into equation (8):

$$\text{minimum mse} = \left(E\left[\epsilon_j^2\right]\right)_{\min} = E\left[d_j^2\right] - \underset{\sim}{W}^{*T}P. \tag{11}$$

THE LMS ALGORITHM

The practical objective of adaptive processes using the adaptive linear combiner is to find a solution to equation (10). An exact solution would require a priori knowledge of the correlation matrixes $\underset{\sim}{P}$ and $\underset{=}{R}$. Since this knowledge is not available, one must find an approximate solution. One way of doing so would be directly by numerical means. This approach, however, would present serious computational difficulties when the number of weights was large or the input data rate high. In addition to the inversion of an $n \times n$ matrix, it would require as many as $n(n+1)/2$ autocorrelation and cross correlation measurements to obtain the elements of $\underset{\sim}{P}$ and $\underset{=}{R}$. Further, this procedure would have to be repeated in most circumstances, where the input signal statistics would be slowly varying.

For these reasons it is more practicable to use other recursive statistical estimation methods in algorithms intended for use with the adaptive linear combiner.

A simple iterative procedure for finding an approximation to the optimal weight vector of the adaptive linear combiner is the LMS ("least mean square") algorithm devised by B. Widrow and M. E. Hoff, Jr. (ref. 6, 7, 8, 9). This algorithm does not require explicit measurements of correlation functions, nor does it involve matrix inversion. Accuracy is limited by statistical sample size, however, since the weight values are based on real-time measurements of the input signals.

The LMS algorithm is based on the method of steepest descent. According to this method the "next" weight vector $\underset{\sim}{W}_{j+1}$ is equal to the "present" weight vector $\underset{\sim}{W}_j$ plus a change proportional to the negative of the instantaneous gradient $\underset{\sim}{\nabla}_j$:

$$\underset{\sim}{W}_{j+1} = \underset{\sim}{W}_j - \mu \underset{\sim}{\nabla}_j, \tag{12}$$

where μ is a parameter that controls stability and rate of convergence. An estimate of the instantaneous gradient $\underset{\sim}{\hat{\nabla}}_j$ is obtained in a crude but efficient manner by assuming that the square of a single error sample ϵ_j^2 is an estimate of the mean square error and by differentiating it with respect to $\underset{\sim}{W}$:

$$\underset{\sim}{\nabla}_j = \left[\frac{\partial \epsilon_j^2}{\partial w_1}, \ldots, \frac{\partial \epsilon_j^2}{\partial w_n}\right]^T_{\underset{\sim}{W}=\underset{\sim}{W}_j} = 2\,\epsilon_j \left[\frac{\partial \epsilon_j}{\partial w_1}, \ldots, \frac{\partial \epsilon_j}{\partial w_n}\right]^T_{\underset{\sim}{W}=\underset{\sim}{W}_j} \tag{13}$$

Since the estimated gradient components are related to the partial derivatives of the instantaneous error with respect to the weight components, which can be obtained by differentiating equation (4), this expression simplifies to

$$\underset{\sim}{\hat{\nabla}}_j = -2\,\epsilon_j \underset{\sim}{X}_j. \tag{14}$$

Equation (12) thus becomes

$$\underset{\sim}{W}_{j+1} = \underset{\sim}{W}_j + 2\mu\epsilon_j \underset{\sim}{X}_j. \tag{15}$$

This algorithm is easily implemented in real-time systems. It requires only two multiplications and two additions per component of $\underset{\sim}{X}$ per input sample.

It has been shown that the gradient estimate used in the LMS algorithm is unbiased and that the expected value of the weight vector converges to the Wiener weight vector when the input vectors are uncorrelated over time (ref. 8, 9, 10, 11).[3] Starting with an arbitrary initial weight vector the algorithm will converge in the mean and will remain stable as long as the parameter μ is greater than zero but less than the reciprocal of the largest eigenvalue λ_{max} of $\underset{\sim}{R}$:

$$1/\lambda_{max} > \mu > 0. \tag{16}$$

[3] *Adaptation with correlated input vectors has been analyzed in references 12 and 13. Extremely high correlation and fast adaptation can cause the weight vector to converge in the mean to something different than the Wiener solution. Practical experience has shown, however, that this effect is generally insignificant.*

Since λ_{max} must be less than the trace of $\underset{\sim}{R}$, which is equal to the total power of the input signal components, the algorithm is unconditionally stable when

$$\frac{1}{\sum_{i=1}^{n} E\left[x_i^2\right]} > \mu > 0, \tag{17}$$

where $E\left[x_i^2\right]$ is the power of the ith signal component.

Figure 2 shows a typical individual "learning" curve—a plot of mean square error as a function of time—representing the dynamic behavior of the LMS algorithm during convergence. Also shown is an ensemble average of 48 learning curves. The ensemble average reveals the underlying exponential nature of the individual curve, which is a sum of exponentials, each associated with a natural mode. The number of natural modes is equal to the number of degrees of freedom (number of weights). The time constant of the pth mode is related to the pth eigenvalue λ_p of the input correlation matrix $\underset{\sim}{R}$ and to the parameter μ by

$$\tau_{p_{mse}} = \frac{1}{4\mu\lambda_p}. \tag{18}$$

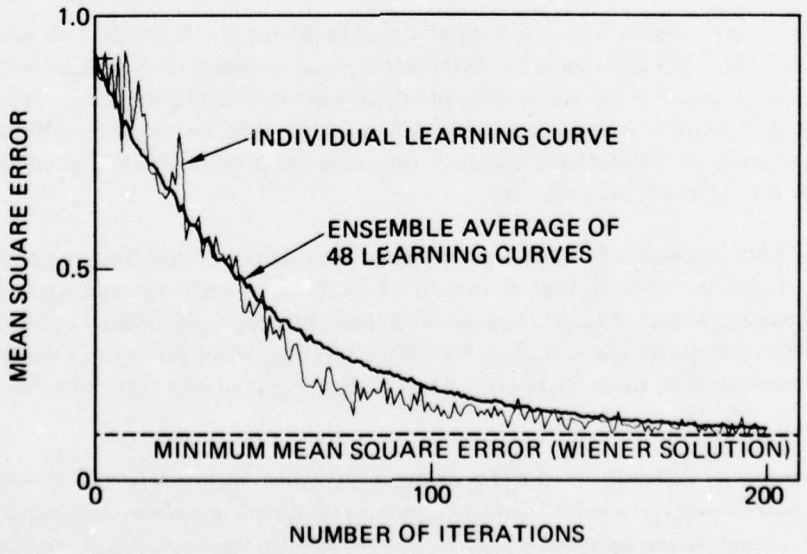

Figure 2. Typical learning curves for LMS algorithm.

In the special case when all eigenvalues are equal, all time constants are also equal. Under these circumstances, which occur when all input signal components are uncorrelated and of equal power, the learning curve is a pure exponential whose time constant[4] is given by

$$\tau_{\text{mse}} = \frac{1}{4\mu\lambda}. \tag{19}$$

The minimum mean square error is ideally realized when the weight vector of the adaptive linear combiner equals the Wiener weight vector $\underset{\sim}{W}^*$. An adaptive algorithm operating in real time with finite speed of adaptation, however, will in most instances not perfectly converge to $\underset{\sim}{W}^*$ because random fluctuations due to gradient estimation error occur in the weight values even at equilibrium. The result is a mean square error that is greater than $\left(E\left[\epsilon_j^2\right]\right)_{\min}$. The amount by which the actual error is greater is called the "excess mean square error." The normalized excess mean square error is in turn defined as the misadjustment M, a dimensionless measure of the difference between actual and Wiener optimal performance:

$$M \triangleq \frac{\text{average excess mean square error}}{\left(E\left[\epsilon_j^2\right]\right)_{\min}}. \tag{20}$$

A good approximate formula for the misadjustment of the LMS algorithm in terms of the number of weights and the time constant of the adaptive process is given by

$$M \cong \frac{n}{4\tau_{\text{mse}}}. \tag{21}$$

Equation (21) shows that the misadjustment can be made arbitrarily small by choosing a long adaptive time constant. Note that for a given time constant misadjustment increases in proportion to the number of weights.[5]

This analysis assumes that the input signal statistics are stationary. If they are slowly varying the LMS algorithm can be thought of as tracking the variation with a delay. Additional mean square error and additional misadjustment will thus occur. It has been demonstrated that under certain conditions the adaptive time constant is optimal when the power of the gradient estimation noise is of the same order of magnitude as the excess mean square error due to the delay (ref. 14).

The LMS algorithm is based on a gradient estimate obtained from a single sample of input data. It has been found that its rate of adaptation is nearly optimal when the eigenvalues of $\underset{\sim}{R}$ are equal (ref. 14). If they are disparate, however, algorithms based on other gradient estimation techniques, such as Newton's method, offer potentially faster convergence to a given level of misadjustment. Several algorithms of this type have recently been described (ref. 16, 17).

---

[4] *If the input signal vector is derived from a tapped delay line, as in an adaptive transversal filter (see below), the time constant can be expressed* $\tau_{mse} = 1/4\mu E[x^2]$, *where x is the input signal to the tapped delay line. Another case of interest occurs when all but two eigenvalues are zero; for example, when the only signal component is a sinusoid. In this case the time constant is given by* $\tau_{mse} = 1/4\mu(n/2)E[x^2]$.

[5] *The topics of time constant and misadjustment are more fully treated in references 8, 9, 14, and 15.*

The LMS algorithm also requires that a weight correction be calculated and applied once each input sample. Such a requirement can be inconvenient in high-frequency applications where analog techniques are used. Further, in some implementations, the $\underset{\sim}{X}$-vector is not available to the adaptive process. Algorithms based on direct gradient estimation or random search techniques are preferable under these circumstances. Unfortunately, however, the misadjustment of these algorithms is proportional to the square of the number of weights and thus for a given rate of adaptation much higher than that of the LMS algorithm (ref. 15).

THE ADAPTIVE FILTER

A choice of x_{ij} for the adaptive linear combiner produces an adaptive filter. The most common choice is to make x_{ij} samples of the same signal at different delays, and the most common method of effecting this choice is to connect the combiner to a tapped delay line to form an adaptive transversal or finite impulse response (FIR) filter. This filter is described in further detail in the following paragraphs, and examples of its application are the subject of the remaining sections of this report.

A block diagram of the adaptive transversal filter is shown in figure 3. Because of the structure of the delay line the input signal vector is

$$\underset{\sim}{X}_j = \left[x_j, x_{j-1}, \ldots, x_{j-n+1}\right]^T. \tag{22}$$

The components of this vector are delayed versions of the input signal x_j.

It is readily observed that the impulse response of the filter of figure 3 is equivalent to the components of its weight vector. Such a filter can thus have any impulse response of length less than or equal to its own length. Further, if it is long enough, it can approximate

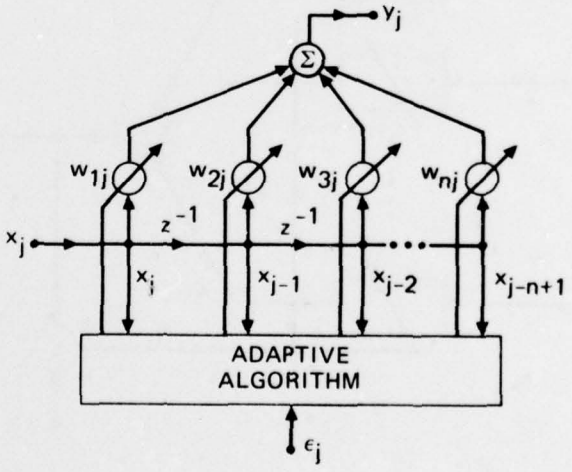

Figure 3. Adaptive transversal filter.

any impulse response at all and hence any frequency response. The penalty for greater length, in addition to greater complexity, is a longer adaptive time constant or greater misadjustment. For many nonstationary applications an optimal length can be found.

A simplified representation of the adaptive transversal filter is shown in figure 4. This representation is useful in depicting adaptive systems that incorporate the filter.

An adaptive system comprising several adaptive transversal filters is shown in figure 5. A system of this kind is useful in processing input signals originating from different sources. It is analytically equivalent to an adaptive linear combiner with multiple inputs instead of a single input, and its properties are fully described by the expressions given in the preceding sections of this report.

Other methods of forming adaptive filters, besides the use of a tapped delay line to provide the $\underset{\sim}{X}$-vector, include the use of serial resistance-capacitance filters of the same time constant (dispersive resistance-capacitance delay line) and parallel-driven filters of different transfer function (ref. 18). In addition, it is possible to derive the components of the $\underset{\sim}{X}$-vector from various physical locations. An example is the connecting of an adaptive linear

Figure 4. Simplified representation of adaptive transversal filter.

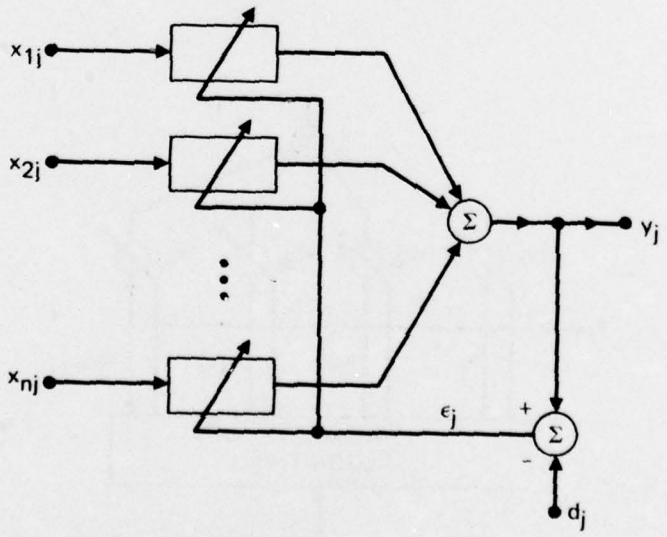

Figure 5. Adaptive filter with multiple input signals.

combiner to the elements of an antenna array to form an adaptive beamformer (ref. 10, 11). Such a beamformer acts as a spatial filter capable of reducing array sensitivity to directional interference. In this respect it resembles the adaptive sidelobe canceller described in one of the following sections of this report.

ADAPTIVE MODELING

Assume that a signal s(t) is applied to a physical system of unknown impulse response h(t) and that it is possible to measure s(t) and the system output s(t)*h(t), where the asterisk denotes convolution. Such conditions occur, for example, when a known signal is transmitted to a receiver over a multipath propagation channel. The adaptive transversal filter described in the preceding sections of this paper can be used to model h(t) by the method shown in figure 6. The signal s(t) or a local replica of it is sampled to form the input x_j of the adaptive filter, and the signal s(t)*h(t) is sampled to form the desired response d_j. The filter output y_j is subtracted from d_j to form the error ϵ_j. The adaptive process minimizes the difference between y_j and d_j to produce the model of h(t). The presence of additive independent noise n(t) in s(t)*h(t) contributes to noise in the weight vector but does not prevent convergence in the mean.

The results of a simple modeling problem simulated on the computer are presented in figure 7. In this problem an adaptive transversal filter incorporating a delay line with four weighted taps was used to model a fixed filter with a transfer function H(z), where z is the unit delay operator, whose roots comprised four zeros. The input signal s consisted of Gaussian noise with a "white" spectrum. Figure 7(a) shows the location in the z plane of the zeros of the fixed filter and the "instantaneous" adaptive zeros in the absence of additive noise.[6] Note that the adaptive model is exact. Figure 7(b) shows the location of the

[6] *In this and the succeeding experiment the zeros and poles of a time-variable filter are defined in a sense that does not have a strict physical interpretation; the filter parameters are "frozen" at any desired point in time and the zeros and poles found in the same way as for a fixed linear filter.*

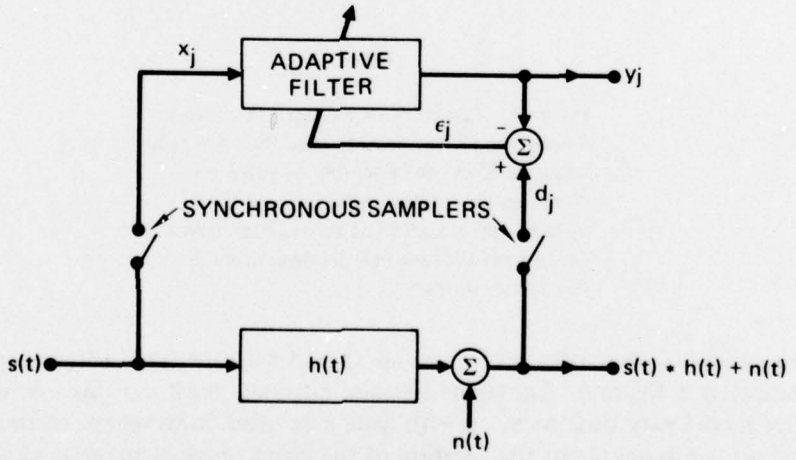

Figure 6. Modeling an unknown dynamic system with an adaptive transversal filter.

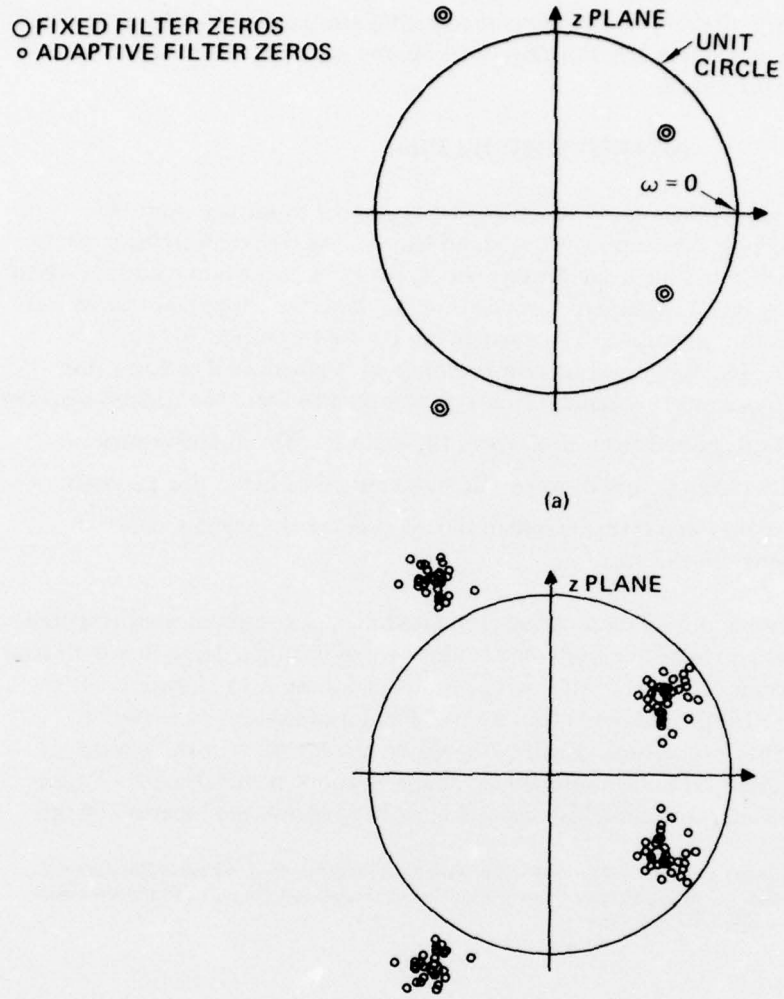

Figure 7. Results of experiment in which a 4-zero fixed filter was modeled by a 4-weight adaptive filter. (a) Location of zeros after convergence without noise in fixed filter output. (b) Location of zeros after convergence with additive independent noise in fixed filter output.

zeros when additive independent noise was combined with the fixed filter output in the manner indicated in figure 6. The signal-to-noise ratio was 0 dB. In this case the zeros of the adaptive model vary their location with time even after convergence of the adaptive process and are scattered about the location of the fixed zeros. The mean location of each group of adaptive zeros, however, is nearly the same as the location of the corresponding fixed zeros. The scattering of the adaptive zeros in this example illustrates the cause of misadjustment, noise in the weight vector.

For an adaptive transversal filter to converge to an exact model of an unknown system the impulse response h(t) of the system must be finite, and the filter's delay line must have a sufficient number of weighted taps to span h(t). If h(t) is not finite an approximate model can be achieved, though this may require a large adaptive system.

The result of a computer simulation in which a 16-weight adaptive transversal filter was used to model a two-pole fixed filter with an infinite impulse response is shown in figure 8. The zeros of the adaptive model are located on a circle at a radius equal to that of the poles of the fixed filter except at frequency $\omega = 0$. Note that the spacing is uniform but that there are no zeros at the location of the poles. This solution represents the best approximation (in the mean square sense) of an all-pole filter by an all-zero adaptive filter.

An adaptive method of uniquely determining both the poles and zeros of an unknown system is described in reference 19. The method shown above could also uniquely determine the poles and zeros of an unknown system if recursive filter coefficients could be directly adapted. This type of adaptation is a current research topic. Further treatment of the techniques and applications of adaptive modeling is provided in references 20 through 26.

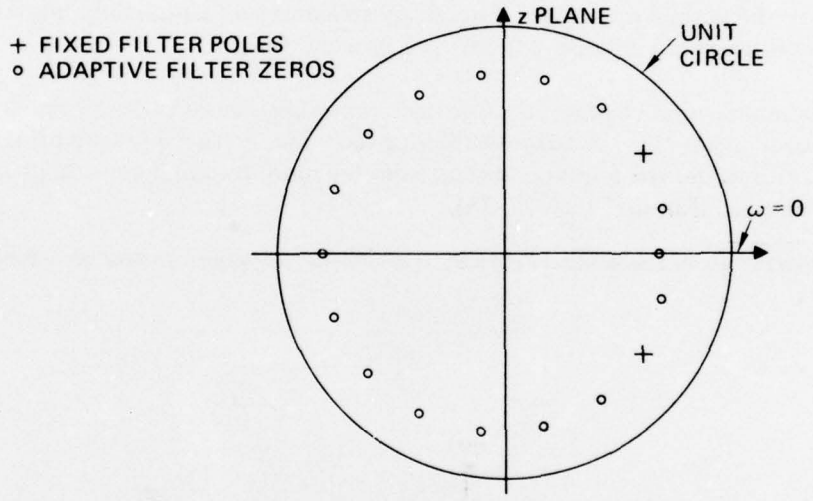

Figure 8. Result of experiment in which a 2-pole fixed filter was modeled by a 16-weight adaptive filter.

ADAPTIVE EQUALIZATION

A frequent problem in communication and data transfer is intersymbol interference caused by multipath propagation. This problem can be solved by a filter placed in series with the propagation channel that produces the inverse of the channel impulse response. Though such a filter normally cannot be designed without prior knowledge of the channel, an approximation can be implemented by adaptive means.

A technique of adaptive channel equalization is illustrated in figure 9. A signal s(t) is transmitted together with a known pilot signal p(t) over a channel with an unknown impulse response.[7] In many cases additive independent noise n(t) is present. The channel output is sampled to form the input x_j to an adaptive filter connected in series with the channel. The desired response d_j is formed by sampling a local replica of the pilot signal p(t). The adaptive process minimizes the difference between the adaptive filter output y_j and the desired response d_j. If a broadband signal is chosen for p(t), a truncated but stable approximation of the optimal equalization filter will be realized.

The results of a digitally simulated channel equalization problem are presented in figure 10. Figure 10(a) shows 8 points of a typical channel impulse response h(t). Figures 10(b) through 10(d) show the equalized channel output y_j, a convolution of channel and equalizer impulse responses, for adaptive filters with 8, 16, and 32 weights respectively. Note that even for a filter with 8 weights the worst sidelobe of the equalized response is 10 dB down. In this experiment Gaussian noise with a white spectrum was used as the pilot signal, and the desired response was delayed by half the delay of the adaptive filter. In a practical system the pilot signal would be a long, repeated pseudorandom noise sequence. The delay in the desired response was necessary to achieve a two-sided impulse response with an adaptive filter whose impulse response is causal and finite.

Communication channel equalization has become one of the most important and widely known applications of adaptive filtering techniques. The approach presented here, entailing a known desired response, differs from the more common approach based on "decision-directed learning" (ref. 27–31).

[7] *The pilot signal may also be transmitted as a preamble; in this case the filter weights are fixed during message transmission.*

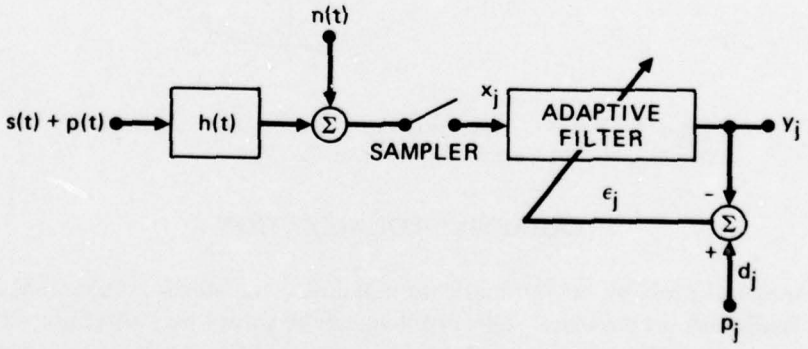

Figure 9. Adaptive equalization of a communication channel.

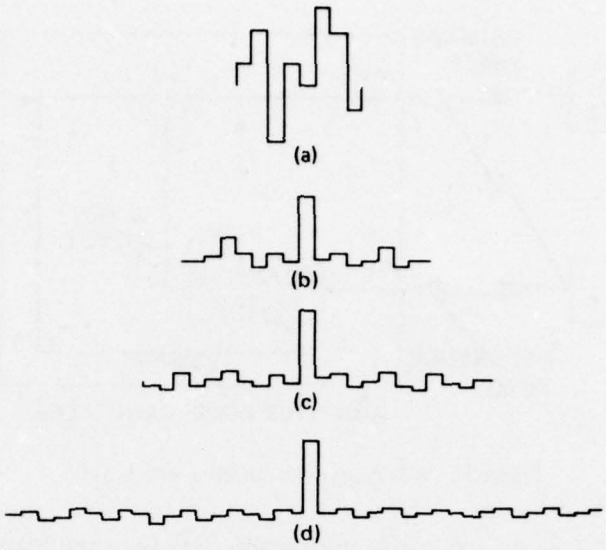

Figure 10. Results of adaptive channel equalization experiment. (a) Channel impulse response. (b) After equalization with 8-weight adaptive filter. (c) After equalization with 16-weight adaptive filter. (d) After equalization with 32-weight adaptive filter.

ADAPTIVE NOISE CANCELLING

Assume a primary sensor receiving a signal contaminated by noise. Imagine that a reference sensor can be located to receive the noise alone. Then it may be possible to filter the output of the reference sensor and subtract it from the output of the primary sensor to obtain signal alone. The difficulty is that the propagation paths from the noise source to the two sensors must be known to design the appropriate filter. These paths are rarely known a priori and are often slowly varying.

The idea of adaptive noise cancelling, as illustrated in figure 11, is to find by adaptive means a filter capable of transforming noise at a reference sensor into noise at a primary sensor. In the system shown the combined signal and noise $s + n_0$ at the primary sensor form the desired response d of the adaptive process, while the related noise n_1 at the reference sensor forms the input x to the adaptive filter. The output y of the adaptive filter is subtracted from d to form the error signal ϵ. This signal is also taken as the output of the canceller.[8]

It might seem that some prior knowledge of the signal s or of the noises n_0 and n_1 would be necessary before the filter could be designed, or before it could adapt, to produce the noise cancelling signal y. A simple argument will show, however, that little or no prior knowledge of s, n_0, or n_1, or of their relationships, either statistical or deterministic, is required.

[8] *A detailed analysis of the adaptive noise canceller is provided in reference 32.*

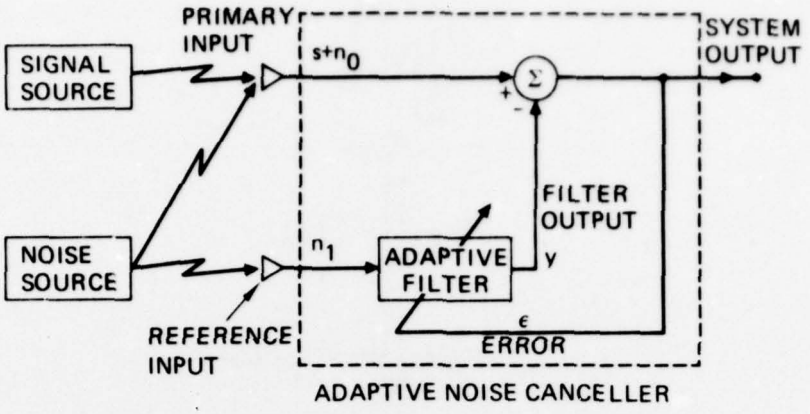

Figure 11. Adaptive noise canceller with inputs.

Assume that s, n_0, n_1, and y are statistically stationary and have zero means. Assume that s is uncorrelated with n_0 and n_1, and suppose that n_1 is correlated with n_0. The output is

$$\epsilon = s + n_0 - y. \tag{23}$$

Squaring, one obtains

$$\epsilon^2 = s^2 + (n_0 - y)^2 + 2s \cdot (n_0 - y). \tag{24}$$

Taking expectations of both sides of equation (24), and noting that s is independent of n_0 and y, yields

$$\begin{aligned} E[\epsilon^2] &= E[s^2] + E[(n_0 - y)^2] + 2E[s \cdot (n_0 - y)] \\ &= E[s^2] + E[(n_0 - y)^2]. \end{aligned} \tag{25}$$

The signal power $E[s^2]$ will be unaffected as the filter is adjusted to minimize $E[\epsilon^2]$. Accordingly, the minimum output power is

$$\min E[\epsilon^2] = E[s^2] + \min E[(n_0 - y)^2]. \tag{26}$$

When the filter is adjusted so that $E[\epsilon^2]$ is minimized, $E[(n_0 - y)^2]$ is therefore also minimized. The filter output y is then a best least-squares estimate of the primary noise n_0. Further, when $E[(n_0 - y)^2]$ is minimized, $E[(\epsilon - s)^2]$ is also minimized, since from equation (23)

$$(\epsilon - s) = (n_0 - y). \tag{27}$$

Adjusting or adapting the filter to minimize the total output power is thus equivalent to causing the output to be a best least-squares estimate of the signal s for the given structure of the adaptive filter and for the given reference input.

To illustrate the application of adaptive noise cancelling two previously described examples from the field of electrocardiography have been chosen (ref. 32). In the first noise cancelling is used to reduce power-line interference obscuring the details of a normal adult electrocardiogram (ECG). In the second it is used to cancel the dominant maternal heartbeat as well as power-line interference in order to record a fetal ECG.

Power-line interference in electrocardiography has various causes, including magnetic induction, displacement currents in leads or in the body of the patient, and equipment interconnections and imperfections. Conventional methods of reducing such interference include the use of proper grounding and twisted pairs during the recording process. An alternative method is to use an adaptive noise canceller to process the ECG recorder signal.

Figure 12 shows the application of adaptive noise cancelling to reduce power-line interference in electrocardiography. The primary input is taken from the ECG preamplifier, and the reference input is taken from a wall outlet. The adaptive filter contains two variable weights, one applied to the reference input directly and the other to a version of it shifted in phase by 90 degrees. The two variable weights, or two "degrees of freedom," are required to cancel the single pure sinusoid.

A typical result of a group of experiments performed with a real-time computer system is shown in figure 13. Figure 13(a) shows the primary input, an electrocardiographic waveform with an excessive amount of power-line interference, and figure 13(b) shows the reference input from a 60-Hz wall outlet. Figure 13(c) is the noise canceller output. Note the absence of interference and the clarity of detail once the adaptive process has converged. In this experiment sample size was 10 bits and sampling rate 1000 Hz.

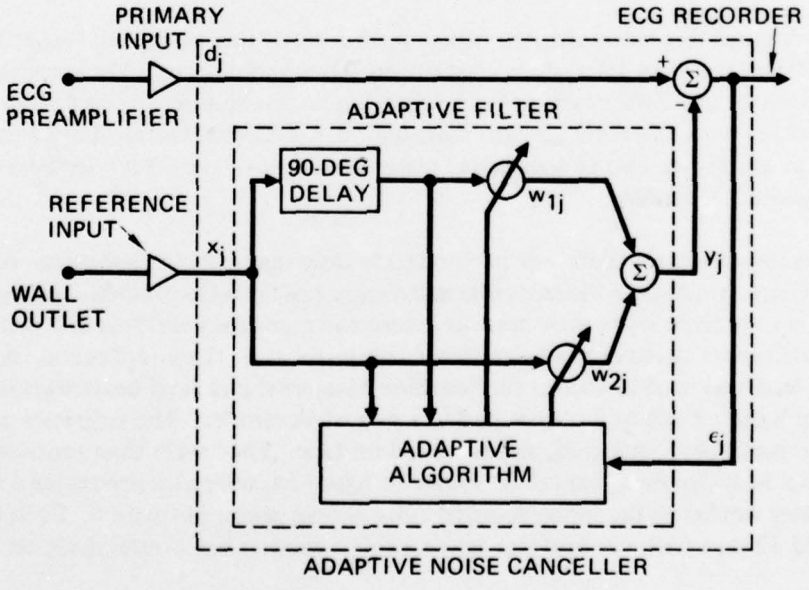

Figure 12. Cancelling power-line interference in electrocardiography.

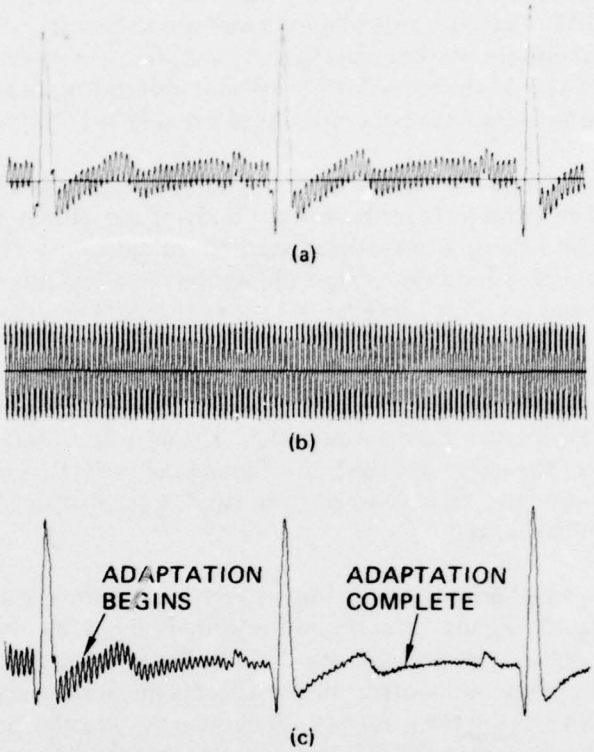

Figure 13. Result of electrocardiographic noise cancelling experiment. (a) Primary input. (b) Reference input. (c) Noise canceller output.

Abdominal electrocardiograms make it possible to determine fetal heart rate and to detect multiple fetuses and are often used during labor and delivery. Background noise due to muscle activity and fetal motion, however, often has an amplitude equal to or greater than that of the fetal heartbeat. A still more serious problem is the mother's heartbeat, which has an amplitude two to ten times greater than that of the fetal heartbeat and often interferes with its recording.

A group of experiments was performed to demonstrate the application of adaptive noise cancelling in reducing the maternal interference in fetal electrocardiography. In these experiments four chest leads were used to record the maternal heartbeat and provide multiple reference inputs containing all significant components of the interference. A single abdominal lead was used to record the combined maternal and fetal heartbeats and provide the primary input. Each lead terminated in a pair of electrodes. The reference and primary inputs were prefiltered, digitized, and recorded on tape. They were then processed in a multichannel adaptive noise canceller, shown in figure 14, which incorporated a four-channel adaptive filter similar to the multiple-input filter shown above in figure 5. Each filter channel had 32 taps with nonuniform spacing (log periodic) and a total delay of 129 ms.

Figure 15 shows the result of a typical experiment. The prefiltering band was 0.3 to 75 Hz and the sampling rate 512 Hz. Baseline drift and 60-Hz power-line interference are

clearly present in the primary input, obtained from the abdominal lead. The interference is so strong that it is almost impossible to detect the fetal heartbeat. The inputs obtained from the chest leads contained the maternal heartbeat and a sufficient 60-Hz component to serve as a reference for both interferences. In the noise canceller output both interferences have been significantly reduced, and the fetal heartbeat is clearly discernible. The noise still evident on the waveform is that due to muscle activity.

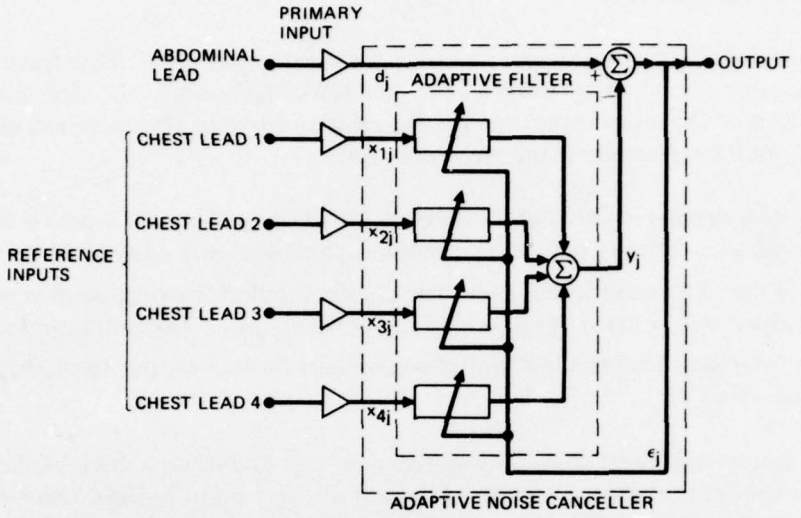

Figure 14. Multiple-reference noise canceller used in fetal ECG experiment.

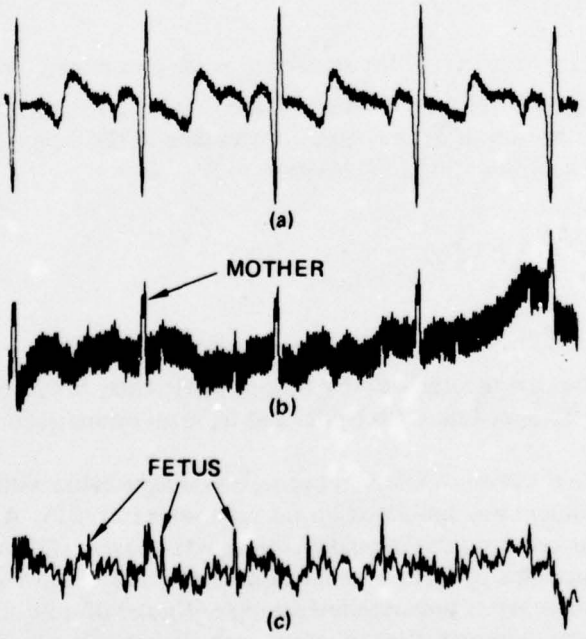

Figure 15. Result of fetal ECG experiment. (a) Reference input (chest lead). (b) Primary input (abdominal lead). (c) Noise canceller output.

ADAPTIVE SIDELOBE CANCELLING

Adaptive noise cancelling can be applied to the output of a receiving antenna array to increase gain substantially against nonisotropic noise, in particular against noise originating from point sources. No prior knowledge of the received signal except for its direction of incidence is required. Sufficient knowledge of the antenna array must be available to allow the formation of crude beams.

An idealized adaptive sidelobe canceller is shown in figure 16. This system includes two beamformers, one of which steers a beam and the other a null in the direction of the signal. The output of the main beamformer is the primary input to the canceller, while the output of the null beamformer is the reference input.

Assume a signal s incident in the steering direction of the main beam of the system of figure 16 and a statistically independent noise n_0 incident on a sidelobe of the main beam. The output of the null beamformer, assuming a perfect null in the steering direction of the main beamformer, will contain a response to the noise n_0 only. The null beamformer output is adaptively filtered and subtracted from the main beamformer output to produce a system output free of noise.

In a practical sidelobe cancelling system a perfect null is not achievable because the properties of the antenna array elements are not ideal. For a multiweight adaptive filter and in the absence of isotropic noise, the output signal-to-noise spectral density ratio of the system of figure 16 is given by

$$(\rho_s/\rho_n)_{out} = \rho_{n_r}/\rho_{s_r}, \tag{28}$$

where ρ_{s_r} and ρ_{n_r} are respectively the signal and noise power spectral density at the null beamformer output (ref. 32).[9] If the ratio of the null beamformer's power gain in the steering direction of the main beamformer to its power gain in the direction of incidence of the noise n_0 is defined as α, equation (28) becomes

$$(\rho_s/\rho_n)_{out} = \frac{1}{\alpha}\frac{1}{(\rho_s/\rho_n)_{in}}, \tag{29}$$

where $(\rho_s/\rho_n)_{in}$ is the free-field input signal-to-noise spectral density ratio. Thus, if the free-field input signal-to-noise spectral density ratio is sufficiently low, a null beamformer is not required, and the reference input can be derived from an omnidirectional sensor ($\alpha = 1$).

To illustrate the level of interference rejection achievable with adaptive sidelobe cancelling a typical problem was simulated on the computer (ref. 32). A circular array consisting of 16 equally spaced omnidirectional elements was chosen. The outputs of the elements were delayed and summed to form a main beam steered at a relative angle of 0 degrees. A simulated signal consisting of uncorrelated samples of noise of unit power was assumed to be incident on this beam. Simulated interference with the same bandwidth and a power of 100

[9] *For a small number of weights inversion of signal-to-noise rather than spectral density ratio occurs.*

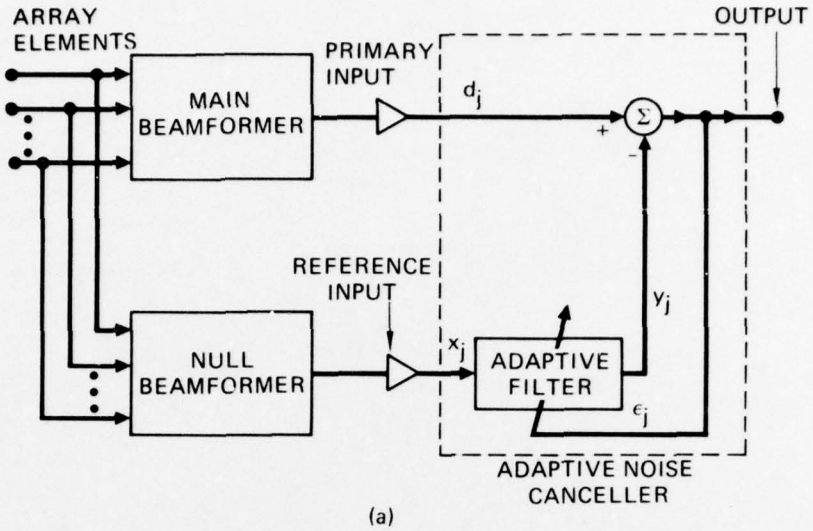

(a)

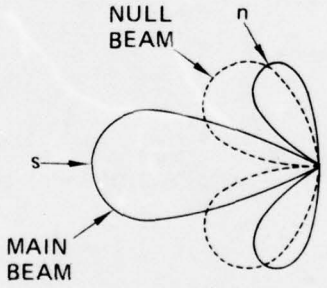

(b)

Figure 16. Adaptive sidelobe canceller. (a) Block diagram. (b) Typical beam patterns with input signals.

was incident at a relative angle of 58 degrees. The array was connected to an adaptive noise canceller in the manner shown in figure 16, except that there was no null beamformer and the output of element 4 was arbitrarily chosen as the reference input. The canceller included an adaptive filter with 14 weights; the adaptive constant of the LMS algorithm was set at $\mu = 7 \times 10^{-6}$.

Figure 17 shows two series of computed directivity patterns, one representing a single frequency of one-fourth the sampling frequency and the other an average of eight frequencies of from one-eighth to three-eighths the sampling frequency. These patterns indicate the

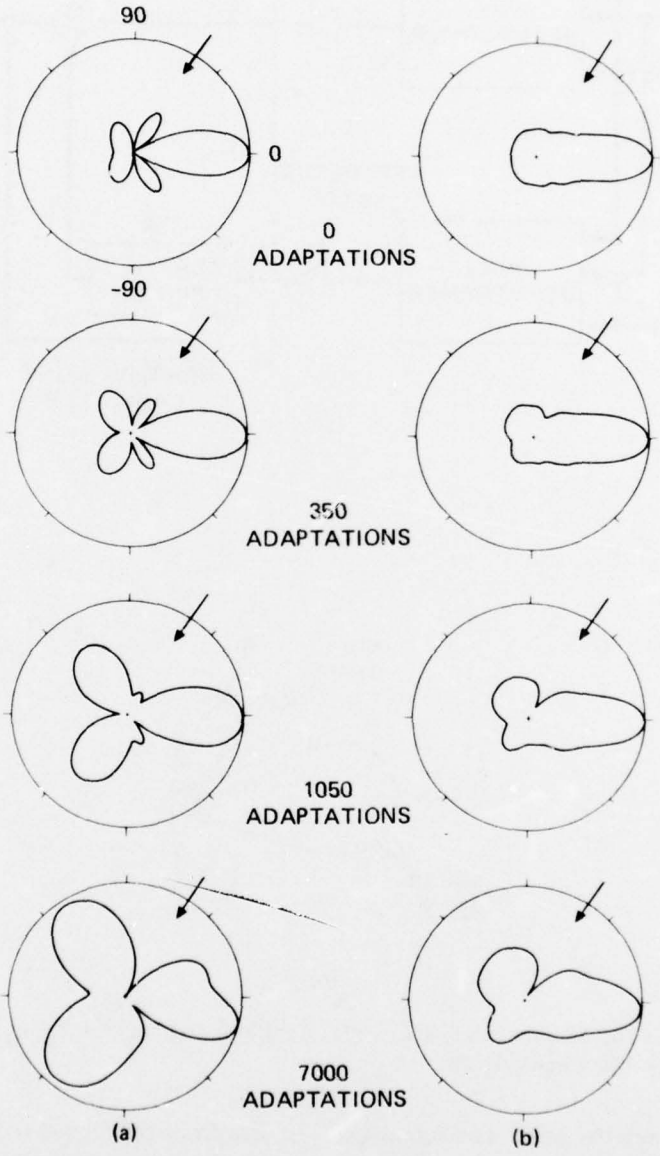

Figure 17. Results of adaptive sidelobe cancelling experiment. (a) Single frequency (one-fourth of sampling frequency). (b) Average of eight frequencies (one-eighth to three-eighths of sampling frequency).

evolution of the main beam and sidelobes as observed by stopping the adaptive process after the specified number of iterations. At the start of adaptation all weights were set at zero, providing a conventional 16-element beam pattern. After adaptation deep nulls have formed in the direction of the interference. Note that a small amount of signal cancellation occurred, as evidenced by the change in sensitivity of the main beam in the steering direction. This change was not unexpected, since the main beam pattern was not constrained by the adaptive process. The signal-to-noise ratio at the system output, averaged over the eight frequencies, was found after convergence to be 20 dB. The signal-to-noise ratio at the single array element was −20 dB. This result is in accordance with the expectation arising from equations (28) and (29), which express output signal-to-noise ratio as the reciprocal of input signal-to-noise ratio.

In the absence of noise or with a narrowband input signal equations (28) and (29) predict poor performance. A number of methods of combating this result, as well as the signal cancellation observed in the foregoing experiment, have been described in the literature (ref. 33–36). In one of these methods, illustrated in figure 18, the null beamformer and single-input adaptive filter used to form and process the reference input in the system of figure 16 are replaced by a multichannel adaptive filter similar to the one shown above in figure 5. The response of this filter, which acts as an adaptive null beamformer, is constrained to be zero in the steering direction of the conventional beamformer by requiring the sum of each column of filter weights to be zero:

$$\mathfrak{F}^T = [0, 0, \ldots, 0], \tag{30}$$

where $\mathfrak{F}$ is defined as the vector of column constraints.[10]

[10] *This constraint, suggested by L. J. Griffiths (ref. 36, private communication), is equivalent to the constraint inherent in O. L. Frost's algorithm (ref. 34). Note that for steering directions other than normal to the array the adaptive filter inputs are derived from the conventional beamformer's delays rather than directly from the elements. Note also that the conventional beamformer's output is delayed by an amount equal to one-half the total delay Δ of the tapped delay line of the adaptive filters or Δ/2; this delay provides the adaptive system with a limited predictive capability.*

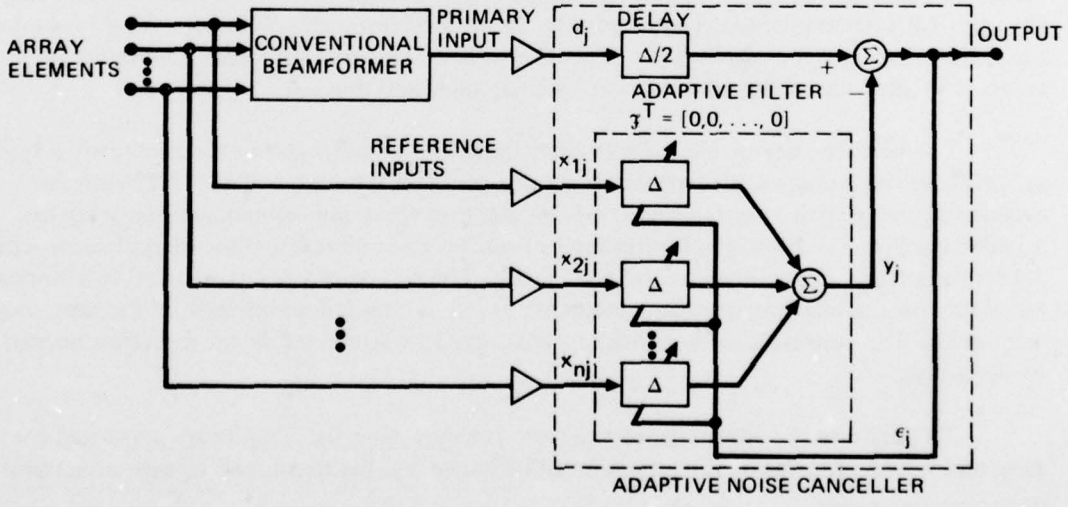

Figure 18. Constrained adaptive sidelobe canceller.

The method of column constraints guarantees a system response in the steering direction of the main beam equal to the response of the conventional beamformer, provided that array properties are ideal. With an actual array, however, a loss of performance with respect to that of the conventional beamformer is experienced because of array gain and phase errors due to irregularities in element placement, transfer function, and near-field effects. This loss is an example of the well-known sensitivity of constrained algorithms to array tolerances (ref. 37).

An alternative method of constrained adaptive sidelobe cancelling has recently been proposed that is relatively insensitive to array gain and phase errors (ref. 15, 38). This method provides a means of rejecting large signals incident on the sidelobes of an array while preserving small narrowband and large as well as small broadband signals incident in the steering direction. In exchange for error tolerance broadband superdirectivity and large narrowband signal reception are lost.

The alternative method is identical to the method already described except in its form of constraint. Instead of the sum of each column of adaptive filter weights the column of individual weights at the middle of each filter and an additional column to either side of it are constrained to be zero. The middle column of zero weights prevents errors in gain from affecting the canceller's performance. The additional column to either side prevents errors in phase from affecting performance.

Operation of the adaptive sidelobe canceller with this method of constraint and broadband signals[11] can be understood by considering equations (3), (6), and (10), which describe the error ϵ, the cross correlation $\underset{\sim}{P}$ between the desired response d and the input signal vector $\underset{\sim}{X}$, and the optimal weight vector $\underset{\sim}{W}^*$. If a signal with a white spectrum is incident on the array, no correlation will exist between any component of the input signal vector and the desired response until the angle of incidence is such that $\delta \geq \delta'$, where δ is the signal delay across the array's aperture and δ' is the delay across the zero-constrained weights of the adaptive filter. In the region $0 < \delta < \delta'$, therefore, no component of $\underset{\sim}{P}$ will be other than zero, and hence $\underset{\sim}{P}$ and the optimal weight vector $\underset{\sim}{W}^*$ will be zero. Under these circumstances the error (or system output) is equivalent to the desired response. When $\delta \geq \delta'$, $\underset{\sim}{P}$ becomes other than zero and the possibility of rejection exists. The effect of array gain or phase errors is to alter the relationship between source angle and delay δ'.

The performance of the error-tolerant sidelobe canceller can be illustrated by a typical problem simulated on the computer. In this problem it is assumed that a directional broadband signal with a white spectrum is incident on the array elements successively over a 180-deg sector.[12] There is a background of uniform nondirectional broadband noise with a white spectrum. Signal-to-noise ratio is 20 dB. The receiving array is assumed to comprise ten elements in a line configuration; element spacing is one-half wavelength at the sampling frequency. The conventional beamformer is assumed to be steered in the direction normal to the array.

To illustrate the advantage of the error-tolerant canceller, results are presented for ideal and nonideal forms of the array described above and for two forms of zero constraint

[11] *Operation with narrowband signals is treated in reference 38.*

[12] *Note that the directional signal is directional interference when not incident on the main lobe of the conventional beamformer.*

on the adaptive filter weights. The two forms of the array are shown in figure 19; in the ideal form the elements are assumed to be in perfect alignment, while in the nonideal form the single elements at each end are assumed to be set forward one-quarter of a wavelength. The two forms of constraint, shown in figure 20, where the rows and columns represent respectively the filters and filter weights and where w and 0 represent respectively the weights controlled and not controlled by the adaptive process, may be described as a "single column

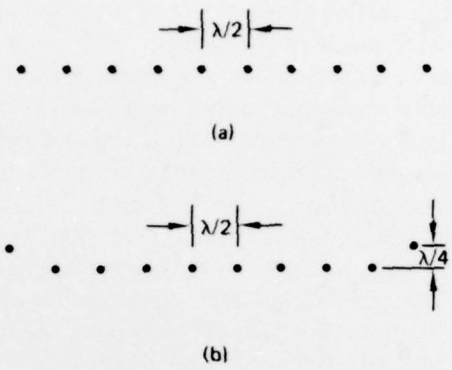

Figure 19. Forms of array used in error-tolerant sidelobe cancelling experiment. (a) Ideal array. (b) Nonideal array.

$$\begin{bmatrix} w & \cdots & w & 0 & w & \cdots & w \\ w & \cdots & w & 0 & w & \cdots & w \\ & & & \vdots & & & \\ w & \cdots & w & 0 & w & \cdots & w \end{bmatrix}$$

(a)

$$\begin{bmatrix} w & \cdots & w & 0 & 0 & 0 & w & \cdots & w \\ w & \cdots & w & 0 & 0 & 0 & w & \cdots & w \\ & & & & \vdots & & & & \\ w & \cdots & w & 0 & 0 & 0 & w & \cdots & w \end{bmatrix}$$

(b)

$$\begin{bmatrix} w & \cdots & w & 0 & 0 & 0 & 0 & 0 & w & \cdots & w \\ w & \cdots & w & w & 0 & 0 & 0 & w & w & \cdots & w \\ & \cdot & & & & 0 & & & & \cdot & \\ & \cdot & & & & & & & & \cdot & \\ & \cdot & & & & 0 & 0 & 0 & & \cdot & \\ w & \cdots & w & 0 & 0 & 0 & 0 & 0 & w & \cdots & w \end{bmatrix}$$

(c)

Figure 20. Weighting coefficient matrices for error-tolerant constrained adaptive sidelobe canceller. (a) Single column-of-zeros constraint. (b) Triple column-of-zeros constraint. (c) "Hourglass" constraint.

of zeros" and a "triple column of zeros." The first, which prevents errors in gain but not in phase from affecting performance, is that suitable for the ideal array. The second, which prevents errors in both gain and phase from affecting performance, is that suitable for the nonideal array. Also shown is a configuration of weighting coefficients that would allow reception of strong broadband signals over a finite and controllable angular sector; in this configuration the zeros are arranged in the form of an "hourglass."

Figure 21 shows simulated directional response patterns indicating the performance of the error-tolerant adaptive sidelobe canceller with the single and triple column-of-zeros constraints. The directional response of the conventional beamformer is also shown for purposes of comparison. Figure 21(a) represents the canceller's response with the ideal array and the single column-of-zeros constraint; note that the beam formed is "superdirective" – that is, much narrower than the conventional beam. Figure 21(b) represents performance with the nonideal array and single column-of-zeros constraint; the beam is severely reduced in sensitivity when array properties are not ideal. Figures 21(c) and 21(d) show the canceller's performance with the triple column-of-zeros constraint. In this case the adaptive beam is closer in width to the conventional beam, but its sensitivity is not significantly affected by the misaligned elements. The new form of constraint thus represents a compromise between directivity and sensitivity to array imperfection, preserving the fundamental capability of an adaptive beamformer to reject interference not incident in the steering direction.

ADAPTIVE PREDICTION, SIGNAL SEPARATION, AND SPECTRAL LINE ENHANCEMENT

Prediction filters can be used to provide estimates of statistically stationary signals at future times. If the statistics of the signal are known a priori, a fixed prediction filter can be designed. In the absence of such knowledge an adaptive predictor that uses measurements of the signal statistics can be implemented.

An adaptive predictor incorporating an adaptive transversal filter is shown in figure 22. The desired response of this system is the unknown but stationary signal whose characteristics are to be predicted at some future time $t + \delta$. The input to the adaptive filter is this signal delayed by the time δ. The filter converges to a weight vector solution that best matches the delayed to the undelayed signal. This solution is duplicated in a slave filter, identical in structure to the adaptive filter, which is used to process the undelayed signal directly and to obtain an optimal least-squares prediction of this signal at time $t + \delta$.[13]

The adaptive predictor of figure 22, as shown in figure 23, can be used without the slave filter as a separator of broadband and narrowband signals. Assume an input signal composed of broadband and narrowband components – that is, components of narrow and wide autocorrelation function. The delay δ will cause decorrelation of the broadband components appearing in the adaptive filter input from those in the desired response. These components will thus appear in the error but not in the filter output. The narrowband components, on the other hand, will not be decorrelated by the delay and will appear in the adaptive filter output.

[13] *More detailed treatment of the adaptive predictor is provided in references 8, 9, 14, and 39.*

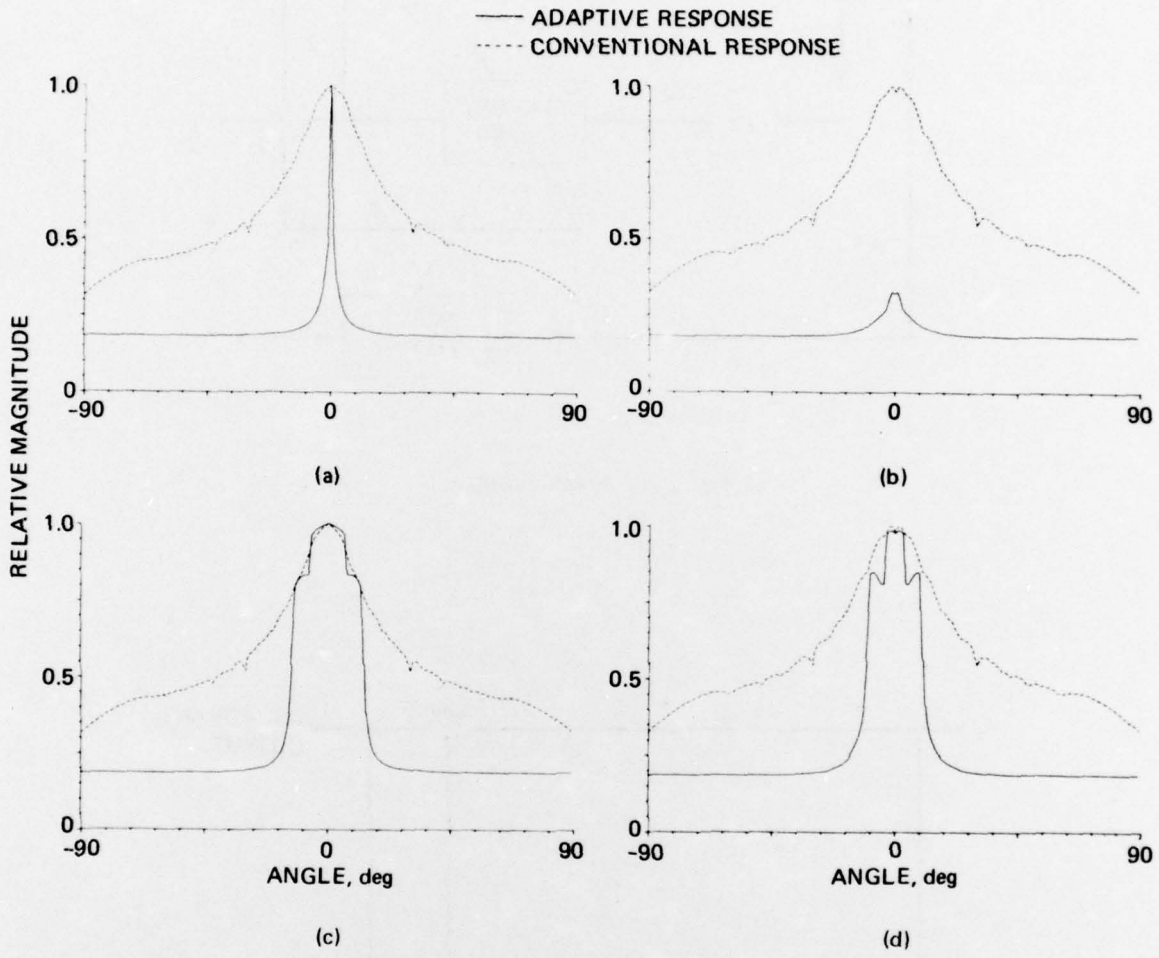

Figure 21. Results of error-tolerant adaptive sidelobe cancelling experiment. (a) Single column-of-zeros constraint, ideal array. (b) Single column-of-zeros constraint, nonideal array. (c) Triple column-of-zeros constraint, ideal array. (d) Triple column-of-zeros constraint, nonideal array.

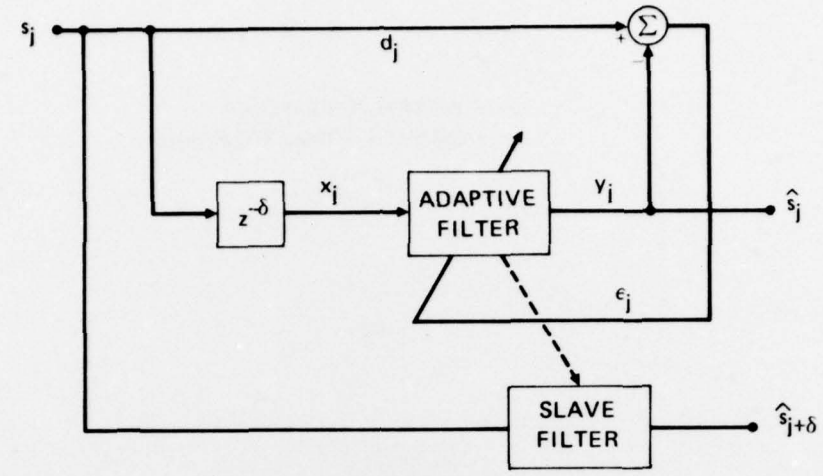

Figure 22. Adaptive predictor.

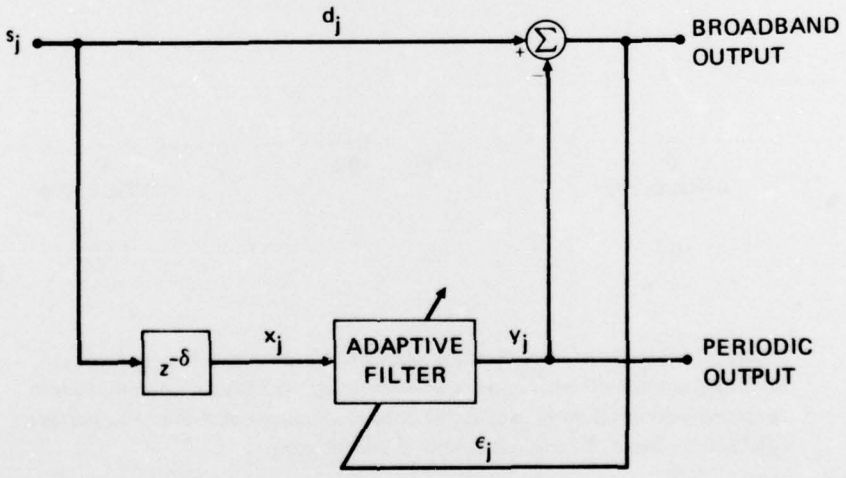

Figure 23. Adaptive signal separator.

Figure 24 presents the results of a computer simulation demonstrating the separation of broadband and periodic signal components (ref. 32). Figure 24(a) shows the input signal, composed of Gaussian noise with a colored spectrum and a sine wave. Figure 24(b) shows the broadband output of the separator, and figure 24(c) shows the periodic output. The broadband and periodic components of the input signal are also shown for comparison with the outputs. Note the close correspondence in form and registration. The correspondence is not perfect only because the adaptive filter was of finite length and had a finite rate of adaptation.

The adaptive signal separator of figure 23 can further be used as a spectral line enhancer capable of detecting narrowband signals of very low amplitude masked by background noise (ref. 32, 40). In this application an estimate of the narrowband components of the input signal is made from the transfer function of the adaptive filter, which is obtained by taking the Fourier transform of the adaptive filter's weight vector $\underset{\sim}{W}$.[14]

Figure 25 presents experimental results, obtained by computer simulation, that compare the performance of the adaptive line enhancer with that of conventional Fourier analysis in detecting a sine wave in Gaussian noise (ref. 40). The results presented show the magnitude of the adaptive filter transfer function and the output power spectral density of the Fourier processor as a function of normalized frequency. The adaptive filter had 128 weights, and the digital Fourier transform had 128 points. The sampling frequency was 1. The number of data samples used was 32,768 in each case. The line enhancer delay was set at 256 samples.

Figure 25(a) shows the performance of Fourier processor and line enhancer against Gaussian noise with a white spectrum. Figures 25(b) and 25(c) show performance against Gaussian noise whose spectrum was 50 percent white and 50 percent colored. The colored noise had a bandwidth of 25 percent and was generated by passing white noise through a filter with two conjugate poles. The colored noise peak was at a frequency of 0.250. Note that the narrowband signal is clearly detected by the line enhancer as well as the Fourier processor even when its frequency is almost the same as that of the colored noise peak. Note also that the response of the line enhancer to the colored noise is negligible.

Figure 26 presents the results of a different but related experiment in which the adaptive separator was used to resolve signals of small amplitude in the presence of a signal of large amplitude (ref. 40). Figure 26(a) shows the power density spectrum of the separator input, which consists of three sine-wave signals whose relative powers are 125, 0.125, and 0.5 and whose relative frequencies are respectively 0.1796875, 0.15625, and 0.421875. These signals are summed with white noise of unit power. The sampling frequency is 1. Note that the first signal is close in frequency to and one-thousand times more powerful than the second signal, which is buried in a sidelobe of the first signal and is not resolvable. The third signal also is not resolvable. Even when the spectrum of figure 26(a) is taken through a Hanning window and plotted on a logarithmic scale, the second signal is undetectable and the third signal though detectable is smaller in amplitude than many of the sidelobes of the first signal. On the other hand, as shown in figure 26(b), when the power density

[14] *The adaptive separator has also been used to implement the maximum entropy filter of reference 41. In this case an instantaneous estimate of the frequency of a narrowband signal of high signal-to-noise ratio is made (ref. 16, 42).*

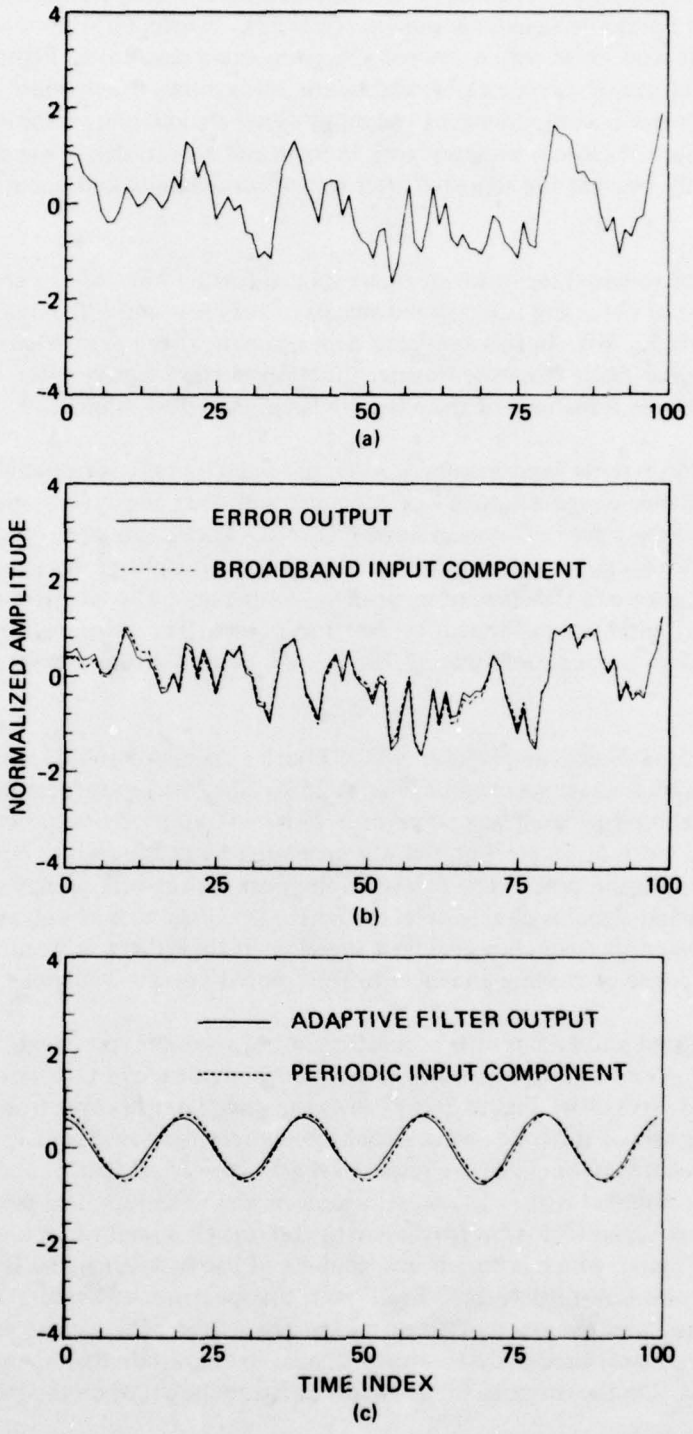

Figure 24. Results of signal separation experiment. (a) Input signal (colored Gaussian noise and sine wave). (b) Error output (colored Gaussian noise). (c) Adaptive filter output (sine wave).

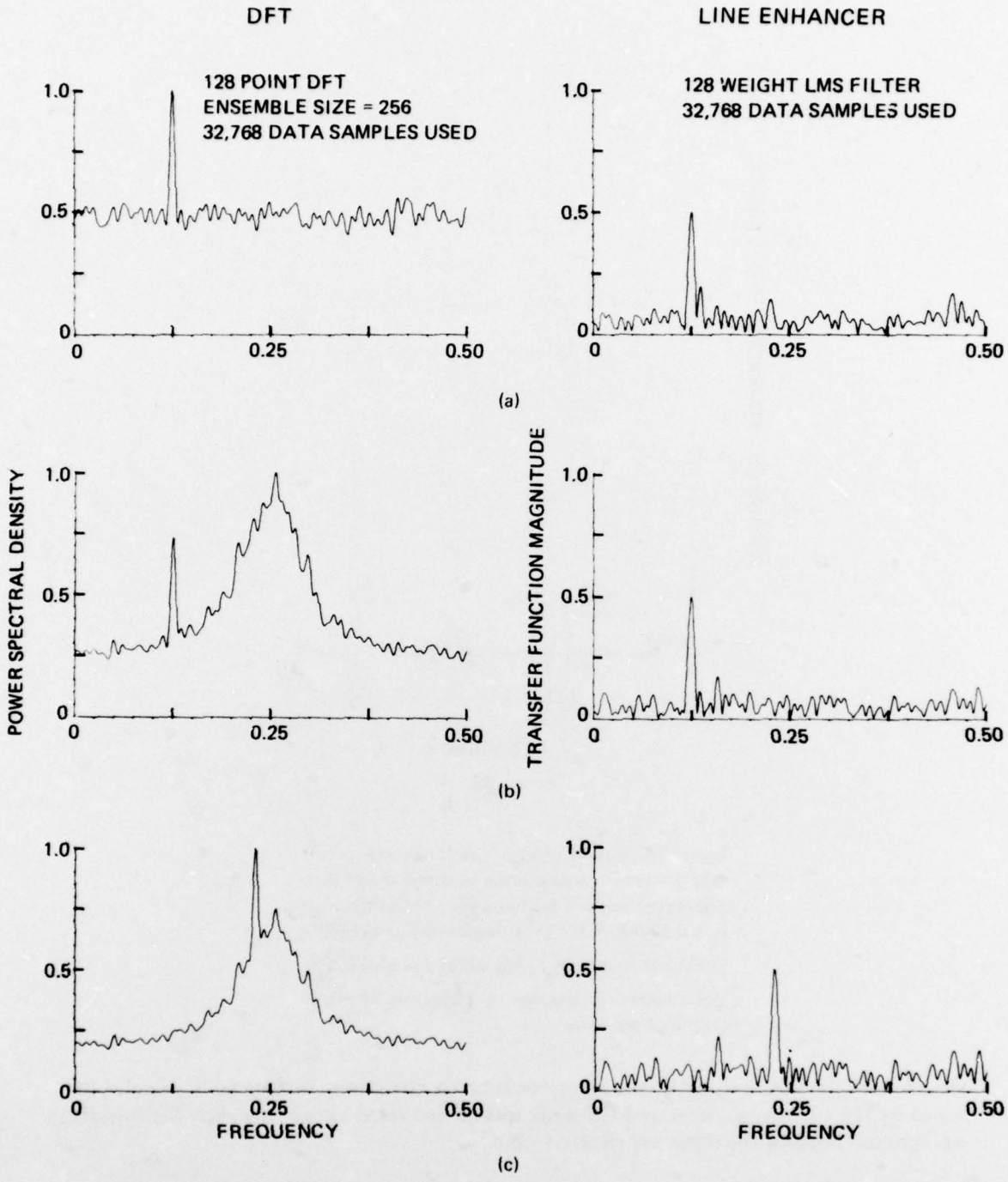

Figure 25. Results of signal detection experiment. (a) Signal of frequency 0.125 in white noise. (b) Signal of frequency 0.125 in 50 percent white and 50 percent colored noise; colored noise peak at frequency 0.250. (c) Signal of frequency 0.220 in 50 percent white and 50 percent colored noise; colored noise peak at frequency 0.250.

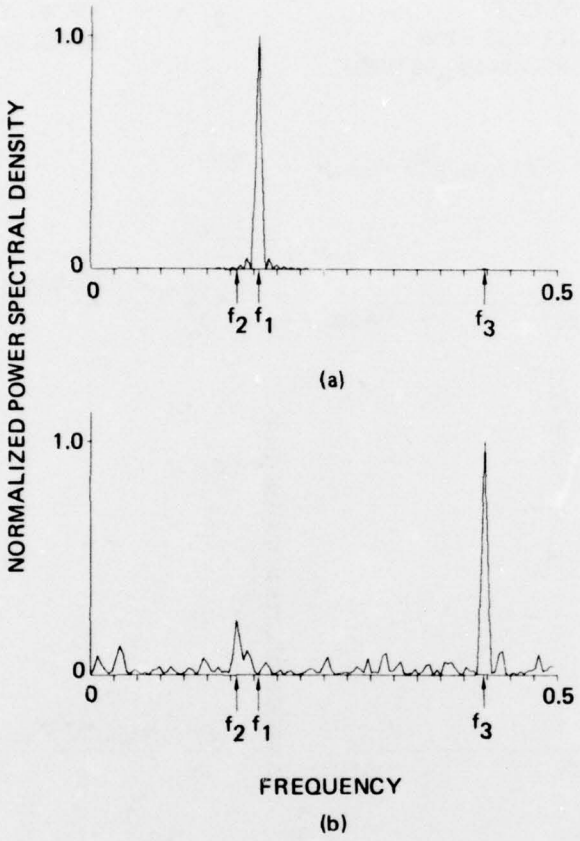

Figure 26. Results of signal resolution experiment. (a) Spectrum of separator input composed of three sine-wave signals of relative power 125 at frequency $f_1 = 0.1796875$, 0.125 at frequency $f_2 = 0.15625$, and 0.5 at frequency $f_3 = 0.421875$ summed in white noise of unit power. (b) Spectrum of error output of separator.

spectrum of the error output of the separator is taken, the strong first signal is absent, cancelled by the adaptive process, and the weak second and third signals as well as the broadband background noise of the input are clearly visible.

The plots of figure 26 are normalized so that full scale corresponds to the largest amplitude point of each. The spectra of the input and error output were taken by digital Fourier analysis; the Fourier transform had 128 points, and there was no ensemble averaging. The 64-weight adaptive filter cancelled the first signal within approximately five cycles of its own frequency; that is, within approximately 30 sample periods. Although an equivalent

result could have been obtained by Fourier analysis alone, it probably would have required substantially more data.

Adaptive techniques, as shown by the results of these experiments, are competitive with conventional digital Fourier analysis in detecting low-level sine waves in noise. Since adaptive techniques are different in implementation from Fourier analysis, they may be more practicable in certain applications. In any case they offer a promising new methodology whose full capabilities remain to be defined.

REFERENCES

1. P. Howells, "Intermediate frequency side-lobe canceller," U. S. Patent 3 202 990, Aug. 24, 1965.

2. S. P. Applebaum, "Adaptive arrays," Special Projects Lab., Syracuse Univ. Res. Corp., Rep. SPL TR 66-1, Aug. 1966.

3. W. F. Gabriel, "Adaptive arrays – An introduction," Proc. IEEE, vol. 64, pp. 239–272, Feb. 1976.

4. N. Wiener, Extrapolation, Interpolation and Smoothing of Stationary Time Series, with Engineering Applications. New York: Wiley, 1949.

5. H. Bode and C. Shannon, "A simplified derivation of linear least squares smoothing and prediction theory," Proc. IRE, vol. 38, pp. 417–425, Apr. 1950.

6. B. Widrow and M. Hoff, Jr., "Adaptive switching circuits," in IRE WESCON Conv. Rec., pt. 4, pp. 96–104, 1960.

7. J. Koford and G. Groner, "The use of an adaptive threshold element to design a linear optimal pattern classifier," IEEE Trans. Inform. Theory, vol. IT-12, pp. 42–50, Jan. 1966.

8. B. Widrow, "Adaptive filters 1: Fundamentals," Stanford Electronics Lab., Stanford Univ., Rep. SU-SEL-66-126, Dec. 1966.

9. B. Widrow, "Adaptive filters," in Aspects of Network and System Theory, R. Kalman and N. DeClaris, Eds. New York: Holt, Rinehart, and Winston, 1971, pp. 563–587.

10. B. Widrow, P. Mantey, L. Griffiths, and B. Goode, "Adaptive antenna systems," Proc. IEEE, vol. 55, pp. 2143–2159, Dec. 1967.

11. R. Riegler and R. Compton, Jr., "An adaptive array for interference rejection," Proc. IEEE, vol. 61, pp. 748–758, June 1973.

12. K. Senne, "Adaptive linear discrete-time estimation," Stanford Electronics Lab., Stanford Univ., Rep. SEL-68-090, June 1968 (Ph.D. dissertation).

13. T. Daniell, "Adaptive estimation with mutually correlated training samples," Stanford Electronics Lab., Stanford Univ., Rep. SEL-68-083, Aug. 1968 (Ph.D. dissertation).

14. B. Widrow, J. McCool, M. G. Larimore, C. R. Johnson, Jr., "Stationary and non-stationary learning characteristics of the LMS adaptive filter," Proc. IEEE, vol. 64, pp. 1151–1162, Aug. 1976.

15. B. Widrow and J. McCool, "A comparison of adaptive algorithms based on the methods of steepest descent and random search," IEEE Trans. Antennas and Propagation, vol. AP-24, pp. 615–637, Sept. 1976.

16. F. J. Harris, "A maximum entropy filter," Naval Undersea Center, San Diego, Calif., Tech. Pub. 441, Nov. 1974.

17. K. H. Mueller, "A new, fast-converging mean-square algorithm for adaptive equalizers with partial-response signaling," Bell Syst. Tech. J., vol. 54, pp. 143–153, Jan. 1975.

18. J. Kaunitz, "General purpose hybrid adaptive signal processor," Stanford Electronics Lab., Stanford Univ., Rep. SEL-71-023, Apr. 1971.

19. P. E. Mantey, "Convergent automatic synthesis procedures for sampled-data networks with feedback," Stanford Electronics Lab., Stanford Univ., Tech. Rep. 6773-1, Oct. 1964.

20. P. M. Lion, "Rapid identification of linear and nonlinear systems," in Proc. 1966 JACC, Seattle, Wash., pp. 605–615, Aug. 1966; also AIAA Journal, vol. 5, pp. 1835–1842, Oct. 1967.

21. R. E. Ross and G. M. Lance, "An approximate steepest descent method for parameter identification," in Proc. 1969 JACC, Boulder, Col., pp. 483–487, Aug. 1969.

22. R. Hastings-James and M. W. Sage, "Recursive generalized-least-squares procedure for online identification of process parameters," Proc. IEE, vol. 116, pp. 2057–2062, Dec. 1969.

23. A. C. Soudack, K. L. Suryanarayanan, and S. G. Rao, "A unified approach to discrete-time systems identification," Int. J. Control, vol. 14, pp. 1009–1029, Dec. 1971.

24. W. Schaufelberger, "Der Entwurf adaptiver Systeme nach der direckten Methode von Ljapunov," Nachrichtentechnik, Nr. 5, pp. 151–157, 1972.

25. J. M. Mendel, Discrete Techniques of Parameter Estimation: The Equation Error Formulation. New York: Marcel Dekker, Inc., 1973.

26. S. J. Merhav and E. Gabay, "Convergence properties in linear parameter tracking systems," Identification and System Parameter Estimation—Part 2, Proc. 3rd IFAC Symp., P. Eykhoff, Ed. New York: American Elsevier Publishing Co., Inc., 1973, pp. 745–750.

27. R. Lucky, "Automatic equalization for digital communication," Bell Syst. Tech. J., vol. 44, pp. 547–588, Apr. 1965.

28. M. DiToro, "A new method of high-speed adaptive serial communication through any time-variable and dispersive transmission medium," in Conf. Record, 1965 IEEE Annual Communications Convention, pp. 763–767.

29. R. Lucky and H. Rudin, "An automatic equalizer for general-purpose communication channels," Bell Syst. Tech. J., vol. 46, pp. 2179–2208, Nov. 1967.

30. R. Lucky et al., Principles of Data Communication. New York: McGraw-Hill, 1968.

31. A. Gersho, "Adaptive equalization of highly dispersive channels for data transmission," Bell Syst. Tech. J., vol. 48, pp. 55–70, Jan. 1969.

32. B. Widrow, J. Glover, J. McCool et al., "Adaptive noise cancelling: Principles and applications," Proc. IEEE, vol. 63, pp. 1692–1716, Dec. 1975.

33. L. J. Griffiths, "A simple adaptive algorithm for real-time processing in antenna arrays," Proc. IEEE, vol. 57, pp. 1696–1704, Oct. 1969.

34. O. L. Frost III, "An algorithm for linearly constrained adaptive array processing," Proc. IEEE, vol. 60, pp. 926–935, Aug. 1972.

35. N. L. Owsley, "A recent trend in adaptive spatial processing for sensor arrays: Constrained adaptation," Signal Processing: Proceedings of the NATO Advanced Study Institute on Signal Processing with Particular Reference to Underwater Acoustics, J. W. R. Griffiths, P. L. Stocklin, and C. Van Schooneveld, Eds. New York and London: Academic Press, 1973, pp. 591–604.

36. L. J. Griffiths, "Adaptive monopulse beamforming," Proc. IEEE (letters), vol. 64, pp. 1260–1261, Aug. 1976.

37. H. Cox, "Sensitivity considerations in adaptive beamforming," Signal Processing: Proceedings of the NATO Advanced Study Institute in Signal Processing with Particular Reference to Underwater Acoustics, J. W. R. Griffiths, P. L. Stocklin, and C. Van Schooneveld, Eds. New York and London: Academic Press, 1973, pp. 619–645.

38. J. M. McCool, "A constrained adaptive beamformer tolerant of array gain and phase errors," Proceedings of the NATO Advanced Study Institute in Signal Processing, Aug. 1976 (forthcoming).

39. J. Makhoul, "Linear prediction: A tutorial review," Proc. IEEE, vol. 63, pp. 561–580, Apr. 1975.

40. B. Widrow, J. Glover, J. McCool, J. Treichler, "Response to letter from D. W. Tufts," Proc. IEEE (forthcoming).

41. J. P. Burg, "Maximum entropy spectral analysis," Presented at the 37th Annual Meeting, Soc. Exploration Geophysicists, Oklahoma City, Okla., 1967.

42. L. J. Griffiths, "Rapid measurement of instantaneous frequency," IEEE Trans. Acoustics, Speech, and Signal Processing, vol. ASSP-23, pp. 209–222, Apr. 1975.


FILM
4